# Non-fungible Token Recommendation: An Intent-Aware Hypergraph Representation Learning Approach

Anonymous Author(s)


## Abstract

The rapid growth of interest in Non-Fungible Tokens (NFTs) has created a growing demand for efficient recommender systems in NFT marketplaces. However, the unique and highly personalized nature of NFTs poses unprecedented challenges for traditional recommendation systems. This paper proposes a novel Intent-aware Hypergraph Representation Learning (IHRL) recommendation model for NFT markets. Inspired by intent-driven interaction patterns in blockchain ecosystems, IHRL models user behavior from an intent perspective, capturing diverse purchasing motivations such as collection, investment, and social showcasing. Our model employs disentanglement techniques to separate and identify distinct intent-specific features, enabling a more precise representation of user preferences across various purchasing motivations. Furthermore, IHRL designs a hypergraph structure to explore higher-order relationships among NFTs. Extensive experiments on a large-scale dataset comprising over 2.6 million Ethereum NFT transactions demonstrate IHRL's significant performance improvements over state-of-the-art baseline methods, validating its effectiveness in the NFT recommendation scenario. The source code of IHRL is available on GitHub: https://anonymous.4open.science/r/IHRL-7F32/.



## CCS Concepts

• **Information systems** → **Recommender systems**.

## Keywords

blockchains, recommender systems, NFT marketplace, hypergraph representation, intent embedding

**ACM Reference Format:**

Anonymous Author(s). 2018. Non-fungible Token Recommendation: An Intent-Aware Hypergraph Representation Learning Approach . In *Proceedings of Make sure to enter the correct conference title from your rights confirmation emai (Conference acronym 'XX)*. ACM, New York, NY, USA, 10 pages. https://doi.org/XXXXXXX.XXXXXXX


## 1 INTRODUCTION

Non-fungible tokens (NFTs) are unique digital assets minted on a blockchain, representing ownership of digital or physical assets. Unlike traditional fungible tokens, NFTs are characterized by their uniqueness and non-fungibility, which has opened up broad application prospects in various domains including art, gaming assets, virtual real estate, and digital collectibles [30]. The unique attributes of NFTs provide creators with novel avenues for artistic expression and monetization and offer collectors and investors unprecedented opportunities for value storage and appreciation. In 2024, the value of NFTs minted and traded on the Ethereum blockchain alone has reached over $7 billion. With the thriving NFT market, there are over 2 million NFT collections and over 1 billion unique NFTs. Efficiently matching users with digital assets that align with their interests has become a pressing challenge [1, 25].

Recommender systems play a crucial role in alleviating information overload. By learning user interest representations, these systems can personalize information filtering and identify relevance, helping users efficiently discover suitable products [20]. However, NFTs, as unique digital assets, fundamentally differ from conventional goods or content. Each NFT possesses its own specific attributes, unique history, and independent value. This high degree of personalization leads to an extraordinary diversity in user preferences for NFTs. Buyers may be motivated by multiple factors, including artistic style, creator reputation, rarity, or potential investment value. Traditional recommendation systems, however, often assume that user behavior reflects similar purchasing motivations, overlooking the complex motivation behind NFT acquisitions. For instance, these systems might struggle to distinguish between purchases made for appreciation and investment purposes.

Recent advancements in blockchain technology have introduced innovative approaches. As blockchain ecosystems mature, interaction models based on user intent are gaining traction. Intent in blockchain refers to a user's specified goal or objective within the blockchain ecosystem [14]. These intents are then delegated to specific resolvers, such as smart contracts or other protocols, for execution without requiring users to detail every step of the implementation process. This intent-driven methodology offers distinctive application value within the NFT market. In each NFT transaction, buyers are able to acquire specific digital assets, while sellers can list them at predetermined price points.

Inspired by the aforementioned intents, we proposed an intent-aware hypergraph representation learning model (IHRL) for NFT recommendation. The core idea of IHRL is to analyze user behavior from the perspective of purchase intents. Unlike traditional methods that only focus on the surface-level buying and selling intents in NFT transactions, IHRL explores deeper user motivations behind trading behaviors, such as collecting, investing, or social showcasing. To avoid interference caused by mixed information, IHRL employs disentangled learning techniques to ensure that the features of each intent can independently and accurately reflect users' true needs. Furthermore, IHRL introduces a hypergraph structure to mine high-order relationships between NFTs. First, IHRL constructs multiple hypergraphs to model purchasing behavior under specific intents. Then, IHRL employs convolutional neural networks to learn NFT embeddings for each hypergraph. Finally, an



*Conference acronym 'XX, June 03–05, 2018, Woodstock, NY*



ACM ISBN 978-1-4503-XXXX-X/18/06
https://doi.org/XXXXXXX.XXXXXXX

attention mechanism is used to combine the embeddings learned from NFTs within the same intent and across different intents. Our main contributions are as follows:

- We propose a novel framework that analyzes user purchasing behavior from the perspective of purchase intents. Combined with disentangled learning techniques, it achieves precise identification of user purchase intents.
- We incorporate a hypergraph structure to uncover intricate connections among NFTs sharing the same intent, while enabling feature propagation across diverse intents.
- Comprehensive benchmarking experiments conducted on real-world NFT datasets demonstrate the state-of-the-art performance of our proposed unified hybrid approach surpassing existing methods in recommendation accuracy.

The remainder of this paper is organized as follows. Section 2 provides background information for a general audience unfamiliar with the NFT field. Section 3 describes the proposed model. Section 4 describes the experimental setup and presents our experimental results. Section 5 discusses the related work. Section 6 concludes our work and outlines future plans.

# 2 BACKGROUND

This section offers background information about the NFT technology, its marketplace and the data.

## 2.1 What Are NFTs?

Non-fungible tokens (NFTs) have distinct attributes that underpin their rapid permeation across digital asset markets. As defined by Bhujel and Rahulamathavan [4], "NFTs are ownership records stored on a blockchain, and they typically represent digital items such as photos and videos." A key differentiator is their non-fungible design whereas cryptocurrencies are fungible. NFTs contain unique properties and metadata encoding specific digital assets, with their content and ownership governed by self-executing smart contracts on the blockchain, which have their terms directly written into code, automatically enforcing agreements and eliminating intermediaries.

Consider digital artworks for example: an artist can create a digital image and issue it as an NFT, effectively producing a certificate of authenticity for that specific digital file. Traditional platforms haven't widely adopted NFT systems due to their established business models and the complex technological shift required. However, NFTs offer artists direct control over their work's distribution and value, potentially disrupting existing intermediaries [31]. "A new blockchain-based technology is changing how the art world works, and changing how we think about asset ownership in the process.". This process transforms easily replicable digital content into a scarce, ownable asset [5, 17]. Notable examples of popular digital arts include Beeple's "Everydays: The First 5000 Days,"[1] a digital collage that sold for $69 million, and the "Bored Ape Yacht Club" series, [2], featuring unique cartoon apes that have become status symbols in some online communities.

The cultural impact of NFTs extends beyond mere ownership [2]. The "CryptoPunks" project, one of the earliest NFT collections, has become a cultural phenomenon, with its pixelated character images serving as profile pictures for celebrities and tech enthusiasts alike. This demonstrates how NFTs can function as digital identity markers and foster community belonging.

## 2.2 The NFT Marketplace

NFT marketplaces are where NFTs are traded. The two largest NFT marketplaces today are Blur[3] and Opensea[4], whose combined market share has been consistently over 90% of all NFT markets.

Intent-driven applications have become increasingly popular in the blockchain industry. Intent in blockchain refers to a user's specified goal or objective within the blockchain ecosystem, which is then delegated to a solver (such as a person, AI, or another protocol) to fulfill, rather than detailing the exact steps needed to achieve that goal [14]. In the NFT marketplace, each transaction is facilitated by the marketplace solver matching a buy order with a sell order, a process enabled through the intent in the blockchain. Each user-submitted buy or sell order contains their transaction intent. The marketplace solvers leverage smart contracts to automatically match these intents, verify the assets of both parties involved, and complete the transaction settlement. Transaction details, including the addresses of the buyer and seller, transaction amount, NFT identifier, and the timestamp of successful matching, are recorded on the blockchain, ensuring transparency and immutability of the data. The transfer of ownership for each NFT is also tracked through the blockchain, guaranteeing the completeness and security of ownership records.

While users in a blockchain marketplace are anonymous, their blockchain addresses will serve as user IDs. These addresses do not correspond to real identifiable users (e.g., a real person may have more than one address). They only identify the transaction parties.

The digital assets as NFTs not only possess unique artistic and collectible value but may also contain utilitarian, investment, political, or social status value [1, 23]. People are drawn to the NFT marketplace for various reasons. For investors, NFTs represent a novel asset class with potential for appreciation. Collectors view them as digital equivalents of traditional collectibles, appreciating their uniqueness and provenance. Artists and creators view NFTs as a way to monetize digital works and maintain ongoing royalties through smart contracts [6]. Moreover, NFTs appeal to those seeking to engage with emerging technologies and participate in new forms of digital culture and commerce [2]. As a result, according to CoinMarketCap's statistics[5], the NFT market in 2023 saw a total annual trading volume of approximately $33 billion, with the market cap remaining above $31 billion by the end of December.

## 2.3 Data Description

As a blockchain application, NFT marketplaces record every successful purchase and cancelled transaction intent on the blockchain, triggering corresponding smart contract events that facilitate the capture and response by marketplace servers and users' frontend interfaces. This means that as analysts, we only need to retrieve historical events to trace all successful purchase records of customers,

[1] See https://opensea.io/assets/ethereum/0x2a46f2ffd99e19a89476e2f62270e0a35bbf0756/40913.

[2] See https://opensea.io/collection/boredapeyachtclub.

[3] https://blur.io

[4] https://opensea.io

[5] https://coinmarketcap.com/nft/

thereby providing a comprehensive and transparent dataset for marketplace analysis and user behavior insights.

Major platforms, including Blur and OpenSea, record the order fulfillment event logs on the Seaport protocol. The Seaport protocol[6] is an open-source smart contract system for NFT markets on the Ethereum blockchain developed by OpenSea. It is designed to be more modular, scalable, and cost-effective in terms of transaction fees compared to traditional NFT marketplace protocols (e.g., the Wyvern protocol). Seaport users can create complex transactions, such as one-time purchases of multiple NFTs, or exchanges of multiple assets in one transaction. Seaport also supports a wider range of use cases, including partial fills, standards-based orders, and tips. Therefore, parsing Seaport gives us the most representative on-chain transaction data.

We extracted all 3,682,913 *OrderFulfilled* records from block 0 to 18,000,000 in the Seaport protocol. Each record represents a completed transaction within the marketplace. The *OrderFulfilled* records contain fundamental transaction characteristics, including timestamp, transaction price, buyer's address, seller's address, the buyer's bid content, and seller's offer content.

## 3 METHODOLOGY

This section introduces our problem formulation and the proposed IHRL model.

### 3.1 Problem Definition

Assume that we are given a set of users $U = \{u_1, u_2, \ldots, u_{|U|}\}$, a set of NFTs $V = \{v_1, v_2, \ldots, v_{|V|}\}$, and their historical interactions. While each NFT is described by a set of features, users are represented by unique addresses only. Our goal is to train a recommender model that infers the probability that a given user $u \in U$ will be interested in buying a given NFT $v \in V$. This model can then provide a personalized ranking of available NFTs for each user.

### 3.2 Overview

As illustrated in Figure 1, IHRL has three modules. The **intent-aware hypergraph learning** module primarily captures high-order relationships among NFTs from the intent perspective, leveraging hypergraph structures. Building upon the learned NFT representations, the **user embedding** module employs a self-attention mechanism to obtain user representations. Finally, the **recommendation** module computes similarity scores between users and NFTs and generates a list of recommended NFTs.

### 3.3 Feature Embedding

For each NFT $v \in V$, we first obtain the vector representation of its ID in the embedding space through an embedding lookup, denoted as $f_v^{ID}$.

Given the significant impact of price on NFT transactions, we further incorporate price information for NFTs. Specifically, we employ a multi-head attention mechanism [28] to process its price sequence. Let $P_v = (p_v^1, p_v^2, ..., p_v^T)$ be the price sequence of NFT $v$ in the previous $T$ transactions. We create the price feature embedding following the multi-head attention mechanism as

$$f_v^{PR} = \text{concat}(head_1, \ldots, head_h) W^O, \tag{1}$$

where concat$(\cdot)$ denotes the concatenation operator. $h$ represents the total number of attention heads, and $head_i$ corresponds to the output of the $i$-th attention head, which is formulated as:

$$head_i = \text{softmax}\left(\frac{QW_i^Q KW_i^{K^T}}{\sqrt{d_k}}\right) V_a W_i^{V_a}, \tag{2}$$

where softmax$(\cdot)$ is the activation function. $W^O$ and $W_i^*$ serve as learnable parameters. The vectors $Q$, $K$, and $V_a$ represent the Query, Key, and Value, respectively, which are fundamental components of the attention mechanism. In our implementation, we define $Q = K = V_a = P_v$, allowing the model to capture complex temporal dependencies within the price data. The scalar $d_k$ denotes the dimensionality of the key vectors, which plays a crucial role in scaling the dot product attention.

Additionally, we consider the trading frequency of NFTs, denoted as $f_v^{TF}$. The trading frequency, defined as the number of transactions involving an NFT, provides insights into its popularity and trading activity, potentially indicating its perceived value in the market. As the trading frequency is already a numerical scalar, we directly incorporate this value into our model.

Finally, we obtain a comprehensive representation for each NFT $v$ by combining the identifier, price information, and trading frequency:

$$\boldsymbol{h}_v = f_v^{ID} \odot \left( W^F \left[ f_v^{PR} || f_v^{TF} \right] + \boldsymbol{b}_F \right), \tag{3}$$

where $W^F$ and $\boldsymbol{b}_F$ are the weight matrix and bias vector, respectively. $||$ represents the concatenation operator. This comprehensive representation allows the model to simultaneously consider the intrinsic features, price dynamics, and market activity of NFTs.

### 3.4 Intent-aware Hypergraph Learning

*3.4.1 Intent Representation.* To effectively capture the nuanced differences in purchase motivations, we propose an innovative approach to model NFTs representations through intent-specific embeddings.

Let $\mathcal{I} = \{1, 2, ..., K\}$ denote the set of $K$ possible intents, such as collecting, investing, or social showcasing. We decompose the NFTs embedding representation $\boldsymbol{h}_v$ into $K$ distinct components, formally expressed as: $\boldsymbol{h}v = \{\boldsymbol{h}_{v,1}, \boldsymbol{h}_{v,2}, ..., \boldsymbol{h}_{v,K}\}$, where $\boldsymbol{h}_{v,k}$ represents the embedding of NFT $v$ in the $k$-th intent space. This disentangled representation enables our model to independently capture NFTs features under each intent, thereby achieving a more detailed and accurate understanding of user behavior.

Based on the assumption that NFTs under the same purchase intent share certain characteristics, we propose aggregating NFTs embeddings within the intent space to construct the representation of the intent itself. Specifically, the embedding representation of the $k$-th intent is defined as follows:

$$\boldsymbol{h}_k = \frac{1}{|V|} \sum_{v \in |V|} \boldsymbol{h}_{v,k}. \tag{4}$$

[6]https://github.com/ProjectOpenSea/seaport

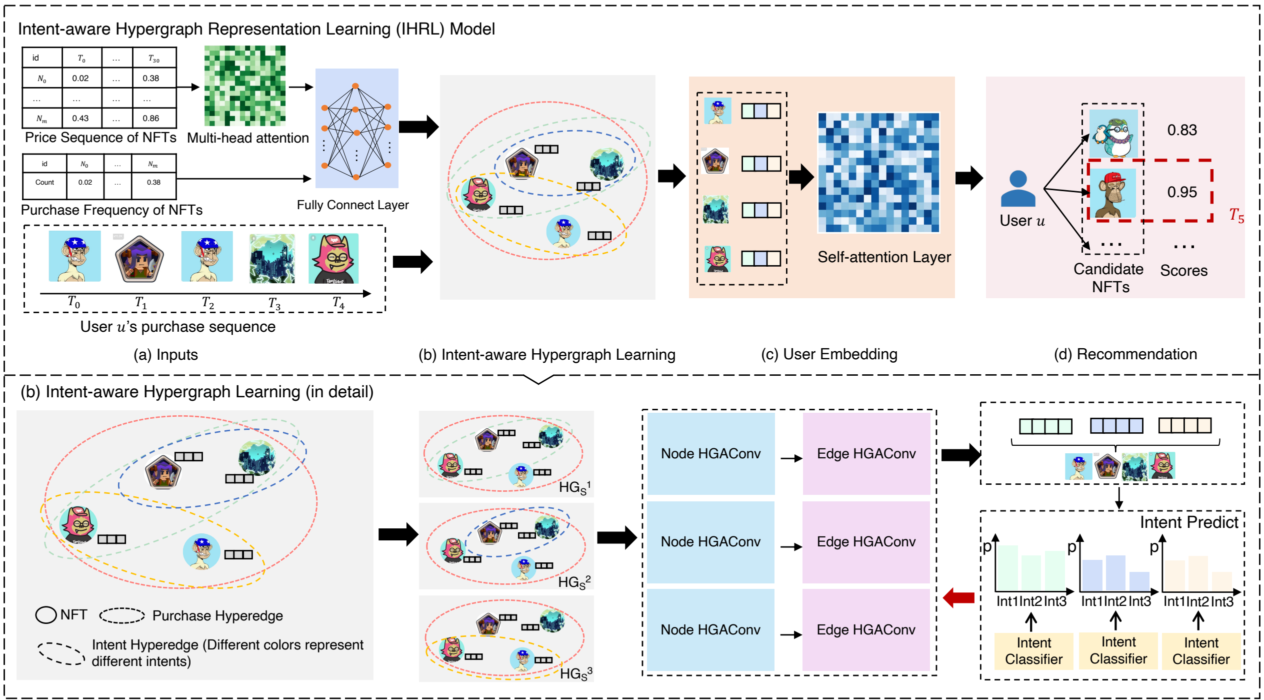


**Figure 1: Overview of the IHRL Model. (1) Top Panel: Intent-aware Hypergraph Representation Model.(2) Bottom Panel: The Intent-Aware Hypergraph Learning Process.**

*3.4.2 Intent-aware Hypergraph Construction.* We propose an intent-aware hypergraph construction method to capture the high-order relationships among NFTs under different intents.

First, we define a hypergraph $\mathcal{G} = (\mathcal{V}, \mathcal{E})$, where $\mathcal{V}$ represents the set of nodes, and $\mathcal{E}$ represents the set of hyperedges. An edge can connect among two or more vertices simultaneously in a hypergraph.

Then, we generate separate hyperedges $\mathcal{E}_k$ for each intent $k$, which connect NFTs with similar intents. The hypergraph structure for each intent $k$ can be formally represented as: $\mathcal{G}_k = (\mathcal{V}_k, \mathcal{E}_k)$. Here, $\mathcal{V}_k$ is the set of NFT nodes, and $\mathcal{E}_k$ is the set of hyperedges constructed based on intent $k$.

Considering the potential noise in the data, we set a threshold to filter intent hyperedges. Specifically, we evaluate the similarity between each intent and each NFT in the corresponding intent space, and only retain the NFT nodes whose similarity to the intent is above the predetermined score $\delta$. The sub-hyperedge connecting NFT $v$ to the $k$-th intent hyperedge can be generated as follows:

$$\varepsilon_{v,k} = \begin{cases} 1 & \text{if } cosine(\boldsymbol{h}_{v,k}, \boldsymbol{h}_k) \geq \delta, \\ 0 & \text{otherwise}, \end{cases} \quad (5)$$

where $\varepsilon_{v,k}$ denotes the sub-hyperedge connecting NFT $v$ to the $k$-th intent hyperedge and $cosine(\cdot)$ represents the cosine function.

*3.4.3 Hypergraph Structure Learning.* We have designed a graph attention convolutional network to update the representations of NFTs. This process consists of two iterative steps: node-to-edge and edge-to-node aggregation. As illustrated in Figure 1 (b), we apply a uniform updating mechanism across all intent-aware hypergraphs. For brevity and ease of understanding, we will focus our discussion on the hypergraph representation learning process within the $k$-th intent space.

**Node to hyperedge.** For each hyperedge $\varepsilon \in \mathcal{E}_k$, we aggregate the feature information of all connected nodes (NFTs). During this process, the attention mechanism dynamically assesses the contribution of each NFT node to the hyperedge representation. This approach enables the model to adaptively adjust the importance weights of different nodes based on the current context and learning task.

The embedding of hyperedge $\varepsilon$ in the $k$-th intent space is updated as:

$$\boldsymbol{h}'_{\varepsilon,k} = AGG_{n2e}(\alpha_{v,\varepsilon,k}\boldsymbol{h}_{v,k} | v \in \boldsymbol{s}_{\varepsilon,k}), \quad (6)$$

where $AGG_{n2e}(\cdot)$ denotes the node-to-hyperedge aggregation operation and $\boldsymbol{s}_{\varepsilon,k}$ represents the set of nodes connected to hyperedge $\varepsilon$. $\alpha_{v,\varepsilon,k}$ is the attention score of node $v$ to hyperedge $\varepsilon$, formulated as:

$$\alpha_{v,\varepsilon,k} = \frac{\exp\left(\text{LeakyReLU}\left(\boldsymbol{q}_{1,k}^{T}(\boldsymbol{h}_{\varepsilon,k} \odot \boldsymbol{h}_{v,k})\right)\right)}{\sum_{v \in \boldsymbol{s}_{\varepsilon,k}} \exp\left(\text{LeakyReLU}\left(\boldsymbol{q}_{1,k}^{T}(\boldsymbol{h}_{\varepsilon,k} \odot \boldsymbol{h}_{v,k})\right)\right)}, \quad (7)$$

where $\boldsymbol{q}_{1,k}$ denotes a learnable hyperparameter, $\odot$ represents the Hadamard product operation, and $\boldsymbol{h}_{\varepsilon,k} = \sum_{v \in \boldsymbol{s}_{\varepsilon,k}} \boldsymbol{h}_{v,k}$ signifies the initial representation of hyperedge $\varepsilon$.

**Hyperedge to node.** We update the representation of each NFT by propagating contextual information from neighboring NFTs through hyperedges. This process can be conceptualized as an information flow from higher-level structures to individual nodes. Similar to the previous stage, we employ an attention mechanism to adaptively adjust the contributions of different hyperedges. The embedding of NFT $v$ in the $k$-th intent space is updated as:

$$\boldsymbol{h}'_{v,k} = AGG_{e2n}\left(\alpha_{\varepsilon,v,k}\boldsymbol{h}'_{\varepsilon,k} | \varepsilon, k \in \boldsymbol{s}_{v,k}\right), \tag{8}$$

where $AGG_{e2n}$ denotes the hyperedge-to-node aggregation operation, $\boldsymbol{s}_{v,k}$ denotes the set of hyperedges connecting to NFT $v$,

$$\alpha_{v,k} = \frac{\exp\left(\text{LeakyReLU}\left(\boldsymbol{q}_{2,k}^T(\bar{\boldsymbol{h}}_{v,k} \odot \boldsymbol{h}'_{\varepsilon,k})\right)\right)}{\sum_{e \in E_v} \exp\left(\text{LeakyReLU}\left(\boldsymbol{q}_{2,k}^T(\bar{\boldsymbol{h}}_{v,k} \odot \boldsymbol{h}'_{\varepsilon,k})\right)\right)} \tag{9}$$

represents the attention score of hyperedge $\varepsilon, k$ for node $v$ for which $\boldsymbol{q}_{2,k}$ is a learnable hyperparameter, $\odot$ represents the Hadamard product operation.

Finally, we obtain the intent-specific embeddings for each NFT $v$, denoted as $\boldsymbol{h}'_v = \{\boldsymbol{h}'_{v,1}, \boldsymbol{h}'_{v,2}, \ldots, \boldsymbol{h}'_{v,K}\}$, where $\boldsymbol{h}'_{v,k}$ represents the NFT's embedding in the $k$-th intent space ($k = 1, 2, \ldots, K$).

*3.4.4 Intent Predict.* To mitigate cross-intent interference and enhance the independence of different intent representations, we design a multi-task intent classification module. For the $k$-th intent space, we employ average pooling to aggregate the learned representations of all NFTs within the space, resulting in a condensed intent-level feature vector. This vector effectively summarizes the overall characteristics of the entire intent space. Subsequently, this aggregated feature is fed into a classifier to predict the probability distribution over all possible intents corresponding to that intent space. This approach not only encourages each intent space to capture unique intent-specific features but also improves the model's generalization capability through a multi-task learning framework. Formally, the intent classification task for the $k$-th intent space can be expressed as:

$$\hat{y}_k = \sigma_I\left(\text{MLP}\left(\frac{1}{|V|}\sum_{v=1}^{|V|}\boldsymbol{h}'_{v,k}\right)\right), \tag{10}$$

where $\hat{y}_k$ represents the predicted probability for the intent $k$. $\text{MLP}(\cdot)$ represents a multi-layer perceptron, which extracts high-level representations from the aggregated intent features. $\sigma_I(\cdot)$ denotes the activation function, where we employ the softmax function to ensure the output is a valid probability distribution. Ultimately, $\hat{y}_k$ represents the predicted probability distribution over intent categories corresponding to the $k$-th intent space. Based on this formulation, the loss function for the intent classification task can be formalized as:

$$\mathcal{L}_{cl} = -\frac{1}{K}\sum_{k=1}^{K}\sum_{i=1}^{K} y_{k,i}\log(\hat{y}_{k,i}) + (1 - y_{k,i})\log(1 - \hat{y}_{k,i}), \tag{11}$$

where $y_{k,i}$ represents the ground truth distribution for the $k$-th intent vector and $i$-th class. $y_{k,i} = 1$ if the $k$-th intent vector belongs to the $i$-th class, and 0 otherwise.

*3.4.5 User Embedding.* Given a user $u \in U$, their historical purchase sequence is denoted as $\boldsymbol{s} = (b_1, b_2, \ldots, b_{|\boldsymbol{s}|})$, where $b_i \in V$ represents the $i$-th NFT they purchased, we construct the user's embedding based on their purchase sequence.

To capture the temporal characteristics of the user's behavior, we integrate positional information into the purchase sequence and denote the enhanced representation of NFT $b_i$ in the user's purchase history as

$$\boldsymbol{h}''_{b_i,k} = [\boldsymbol{h}'_{b_i,k} || \boldsymbol{p}_i], \tag{12}$$

where $\boldsymbol{p}_i$ denotes the positional encoding of the $i$-th purchased item and $||$ represents the concatenation operator. In other words, the NFT $b_i$'s representation in each intent space is attached to a position encoding to incorporate the sequence information of this NFT in this user's purchase experience.

To capture user preferences across different intent spaces, we employ a self-attention mechanism to learn the representation of user $u$ in each intent space. This approach allows the model to dynamically focus on key information within the sequence while considering complex interactions between items. The representation of user $u$ in the $k$-th intent space can be formalized as,

$$\boldsymbol{h}_{u,k} = \sum_{i=1}^{|s|} a_{b_i,k} \cdot \boldsymbol{h}''_{b_i,k}, \tag{13}$$

where $a_{b_i,k}$ represents the importance of the NFT $b_i$ to the user within the intent space $k$, calculated as

$$a_{b_i,k} = \frac{\exp\left(\frac{q_{b_i,k}^T k_{b_i,k}}{\sqrt{d_{\text{dim}}}}\right)}{\sum_{i=1}^{|s|}\exp\left(\frac{q_{b_i,k}^T k_{b_i,k}}{\sqrt{d_{\text{dim}}}}\right)} \times \boldsymbol{h}'_{b_i,k}, \tag{14}$$

where $q_{b_i,k}$, $k_{b_i,k}$, and $v_{b_i,k}$ represent the query, key, and value matrices, respectively. Here, we initialize $q_{b_i,k}, k_{b_i,k}, v_{b_i,k}$, and $h''_{b_i,k}$ to the same value. The parameter $d_{dim}$ is the dimension of $q_{b_i,k}$.

Finally, the intent-aware representation of the user $u$ can be denoted as $\boldsymbol{h}_u = \{\boldsymbol{h}_{u,1}, \boldsymbol{h}_{u,2}, \ldots, \boldsymbol{h}_{u,k}\}$, where $\boldsymbol{h}_{u,k}$ represents the user's embedding in the $k$-th intent space.

## 3.5 Recommendation

Based on the constructed user representations $\boldsymbol{h}_u$ and NFT representations $\boldsymbol{h}_v$, we can compute matching scores between any given pair of user $u \in U$ and NFT $v \in V$ as

$$\hat{y}_{ub_i} = \sum_{k=1}^{K} \boldsymbol{h}_{u,k} \cdot \boldsymbol{h}_{b_i,k}. \tag{15}$$

To optimize the model parameters, we adopt Binary Cross-Entropy (BCE) as our objective function. BCE can effectively solve binary classification problems, particularly in the context of implicit feedback scenarios in recommender tasks. Specifically, our objective function is defined as

$$loss = -\sum_{(u,v)} y_{uv}\log(\hat{y}_{uv}) - (1 - y_{uv})\log(1 - \hat{y}_{uv}), \tag{16}$$

where $y_{uv}$ denotes the ground truth distribution of the interaction between user $u$ and NFT $v$, which takes value 1 if NFT $v$ appears in the purchase sequence of user $u$, and 0 otherwise.

### 3.6 Complexity Analysis

In this section, we present a detailed analysis of the model's time complexity. The complexity of our proposed model can be decomposed into three key modules. i) In the embedding module, the complexity of embedding lookups is $O(B|s|d)$, where $B$ is the batch size. ii) In the intent-aware hypergraph learning Module, the complexity is $O(BKN(d+log(N))+BKNEd)$, where $N = |V|$ is the total number of NFTs and $d$ is the embedding dimension of NFTs. However, we use the Sparse matrix instead of the full matrix in hypergraph structure learning. This significantly reduces the computational complexity and memory requirements. Therefore, the complexity is reduced from $O(N * E)$ for dense matrices to $O(nnz)$, where $nnz$ is the number of non-zero elements in the sparse matrix. iii) In the recommendation module, the complexity is $O(BNd)$. To sum up, the complexity of IHRL is $O(B|s|d + BKN(d + log(N)) + BKnnzd + BNd) \approx O(Nlog(N))$.

## 4 EXPERIMENTAL EVALUATIONS

### 4.1 Settings

*4.1.1 Data Preparation.* In this experiment, we utilized a dataset of NFT transactions from the Ethereum blockchain, spanning from June 2022 to November 2023. The data was collected from five Seaport smart contracts. We focused on the OrderFulfilled events, which capture detailed transaction information including order hash, buyer and seller addresses, recipient address, and specifics of the NFTs and tokens involved in each transaction. The detailed data acquisition process and data descriptions can be found in Appendix A.

To ensure data quality and representativeness, we applied two filtering criteria: NFTs with at least 20 transactions and users with a minimum of 2 transactions were retained. After the preprocessing steps, our dataset includes a total of 112,398 users, with an average of 23.3 transactions per user. There are 2,130,719 items, with an average of 1.4 transactions per item. There are a total of 2,613,617 transactions, resulting in a data sparsity of 99.9989%. We split the dataset into training (80% users) and test (20% users) sets, and report results based on the test set.

*4.1.2 Benchmark Models.* We compare IHRL, our proposed NFT recommendation model, against several baselines. They are described as follows.

**GRU4Rec**: GRU4Rec is a session-based recommendation model using recurrent neural networks [12], capturing item sequence dependencies throughout entire sessions via GRU units.

**SASRec**: SASRec employs a self-attention mechanism for sequential recommendation [15], adaptively focusing on key items in users' historical behaviors and effectively capturing both long-term and short-term patterns to predict the next item.

**LightGCN**: LightGCN is a simplified graph convolutional network model designed for collaborative filtering [11]. It removes nonlinear activations and feature transformations from GCN, retaining only neighborhood aggregation and message passing.

**SINE**: SINE is a sequential recommendation model that captures users' diverse interests through sparse interest extraction and interest aggregation modules, predicting user intents [27]. It achieves more accurate recommendations through large-scale concept modeling and end-to-end learning.

**CORE:** CORE is a session-based recommendation model addressing the inconsistency between session and item embeddings [13]. It unifies the representation space for sessions and items, improving recommendation accuracy and efficiency.

*4.1.3 Evaluation Metrics.* We compare several commonly used performance metrics measuring recommendation accuracy and diversity. For accuracy, we consider Recall and Mean Reciprocal Rank (MRR). For diversity, we consider Index Coverage (IC). For all these metrics, higher values are desired. For these rank-based performance metrics, we consider top 5, 10, 15, and 20 results.

**Recall** is a measure for computing the fraction of relevant items out of all relevant items.

$$\text{Recall@K} = \frac{1}{|U|}\sum_{u\in U}\frac{|\hat{R}(u)\cap R(u)|}{|R(u)|} \tag{17}$$

where $|R(u)|$ represents the item count of $R(u)$

**Mean Reciprocal Rank (MRR)**, as a single-query metric assessing ranking quality, is defined as:

$$\text{MRR} = \frac{1}{|Q|}\sum_{i=1}^{|Q|}\frac{1}{\text{rank}_i}, \tag{18}$$

where $\text{rank}_i$ refers to the rank position of the first relevant document for the $i^{th}$ query in $Q$. MRR is informative when considering user satisfaction for an individual query.

**Index Coverage (IC)** measuring model coverage and diversity, IC calculates the percentage of items from the overall database appearing in recommendations:

$$\text{IC} = \frac{|\bigcup_{u\in U}\mathcal{I}_u|}{|\mathcal{I}|}, \tag{19}$$

where $\mathcal{I}_u$ and $\mathcal{I}$ are the recommended and overall catalogs, respectively. Higher values are desired as they indicate less redundancy.

*4.1.4 Platform and Implementation.* Our experiments were conducted on a server with dual AMD EPYC 7763 64-core processors and 2TiB of memory. The server has over 20TiB of solid-state drive (SSD) storage to support blockchain nodes and a database. It also has 8 NVIDIA GeForce RTX 3090 GPUs, enabling rapid performance of deep learning tasks on the data.

For implementation, we utilized PyTorch as the core framework along with the RecBole library which provides various reusable components for recommendation models. The flexible design of RecBole allowed rapid iteration and validation of various models.

We also leveraged Docker to deploy and run an Archive Ethereum node for acquiring raw blockchain data. Smart contracts and transactions on Ethereum served as the foundation for extracting NFT interaction traces. We further leverage blockchain ETL tools[7] to parse the chain data into structured ClickHouse database tables. This optimized storing and querying of the voluminous data during the stages of data cleaning and feature engineering.

[7]The ETL toolkit is available on Github, but the URL is not provided due to double-blind anonymity requirement.

**Table 1: Performance Comparison.**

| Metric | Recall (%) | | | | MRR (%) | | | | IC (%) | | | |
|---|---|---|---|---|---|---|---|---|---|---|---|---|
| N Value | 5 | 10 | 15 | 20 | 5 | 10 | 15 | 20 | 5 | 10 | 15 | 20 |
| GRU4Rec | 11.60 | 18.32 | 23.85 | 28.15 | 6.02 | 6.89 | 7.31 | 7.55 | 23.55 | 36.60 | 46.30 | 53.49 |
| SASRec | 48.59 | 57.93 | 63.75 | 67.29 | 37.92 | 39.13 | 39.58 | 39.78 | 25.97 | 39.45 | 48.89 | 56.16 |
| LightGCN | 41.00 | 47.47 | 52.67 | 55.90 | 30.41 | 31.35 | 31.63 | 31.88 | 16.37 | 25.46 | 32.10 | 37.32 |
| SINE | 61.81 | 64.78 | 67.05 | 68.99 | 53.78 | 54.19 | 54.30 | 54.36 | 11.37 | 16.02 | 20.06 | 24.03 |
| CORE | <u>72.17</u> | <u>75.35</u> | <u>76.76</u> | <u>77.67</u> | <u>64.17</u> | <u>64.61</u> | <u>64.72</u> | <u>64.77</u> | <u>28.28</u> | <u>42.18</u> | <u>51.00</u> | <u>57.82</u> |
| **IHRL** | **74.04** | **79.42** | **81.48** | **82.78** | **63.91** | **64.63** | **64.80** | **64.86** | **30.78** | **47.26** | **58.18** | **65.67** |
| IHRL (without Intent) | 68.06 | 73.68 | 77.26 | 78.89 | 57.67 | 58.42 | 58.70 | 58.79 | 28.52 | 43.36 | 53.59 | 61.07 |
| IHRL (Avg Session) | 61.25 | 67.68 | 71.13 | 73.40 | 51.37 | 52.22 | 52.50 | 52.62 | 14.94 | 23.38 | 29.96 | 35.52 |

Our model employs the following hyperparameter settings: learning rate of 0.001, batch size of 512, intent count of 5, embedding size of 320, and 2 attention heads. These parameters were determined through grid search optimization.

## 4.2 Results

Since our recommender system is an early work in the field, to better demonstrate the practical significance of our research, our experimental results will be presented around the following research questions (RQs):
**RQ1** How much improvement in performance can our model achieve compared to the baseline model?
**RQ2** To what extent do the individual components of the proposed model contribute to its overall recommendation performance?
**RQ3** How do variations in key model parameters affect the efficacy of the recommender system?

*4.2.1 RQ1: Benchmark.* We compare the performance of IHRL with the benchmark methods and show results in Table 1. We can see that IHRL marks a significant performance improvement in the recommendation capabilities. While both CORE and IHRL leverage sequential data to incorporate contextual information in modeling user characteristics, IHRL achieves a marked improvement in performance, particularly in terms of Recall. This enhancement is especially significant given that CORE already outperforms other baseline models in the comparison. This can be attributed to the following factors: (1) Refined modeling of purchase intents. Our model employs disentangled learning techniques to more accurately capture and differentiate users' diverse purchase intents. This approach enables the model to gain a deeper understanding of the motivations underlying user behaviors, thereby facilitating more precise recommendations. (2) Understanding Complex Relationships Among NFTs. Our model benefits from hypergraph representation learning techniques, enabling it to handle relationships among NFTs that extend beyond pairwise associations. Through the disentangled learning, combined with various purchase intents, our model can more accurately and effectively model NFT representations and generate more relevant recommendations.

*4.2.2 RQ2: Ablation Study.* We systematically evaluate the impact of key components on the model's performance to answer RQ2. Specifically, we examined two main aspects: (1) the role of intent consideration in the model's decision-making process, and (2) the effect of modifying the user representation generation method. In the latter case, we replaced the self-attention mechanism with a simple averaging approach. These ablation studies aimed to isolate the contributions of individual components and provide insights into their relative importance within the overall model architecture.

Results are shown in the last two rows of Table 1. We observe that removing the self-attention mechanism results in the most substantial performance degradation. This underscores the crucial role of considering contextual information and temporal dynamics in effectively modeling complex user preferences. Although the impact of removing intent consideration on model outcomes is comparatively smaller, there is a notable decline in model performance across all metrics, including Recall, MRR, and IC. These significant differences highlight the critical function of intent modeling in capturing nuanced user preferences and behaviors within the NFT market.

*4.2.3 RQ3: Parameter Sensitivity Analysis.* A sensitivity analysis was performed on the primary hyperparameters of our model. We focus on two crucial parameters: the number of intents and the dimensionality of the feature space. We systematically varied the number of intents, testing values of 1, 2, 4, 5, and 8. Simultaneously, the dimensionality was adjusted, exploring settings of 160, 320, and 640. Such a meticulous examination allowed us to gauge the model's responsiveness to parameter adjustments and identify potential optimal configurations. By assessing the model's performance across these varied settings, we sought to understand the robustness of our approach and its sensitivity to hyperparameter choices.

Table 2 in the Appendix elucidates the significant influence of intent quantity on model efficacy. As the number of intents grows, the model's performance exhibits a non-monotonic trend across three key metrics: Recall, MRR, and IC. This trend is characterized by initial improvement followed by a subsequent decline. The model achieves optimal performance across all evaluation metrics when the number of intents is set to 5. Specifically, with 5 intents, the model attains a Recall@20 of 82.78%, an MRR@20 of 64.86%, and an IC@20 of 65.67%, substantially outperforming configurations with other intent quantities. Notably, when the number of intents increases from 5 to 8, a marked decline is observed across all metrics, suggesting that excessive granularity in categorizing user purchase intents may introduce noise, potentially compromising the model's predictive power.

Table 3 in the Appendix provides a comprehensive analysis of the impact of embedding dimension size on model performance. As the dimension increases from 80 to 320, we observe a consistent and significant improvement across all performance indicators. This trend is particularly pronounced for the 320-dimensional embeddings, which achieve peak performance across all metrics. However, this upward trajectory does not persist indefinitely. When the dimension is further increased to 640, model performance exhibits a decline. This pattern suggests that while higher dimensionality can capture more complex feature interactions, excessively high dimensions may introduce noise or lead to overfitting, ultimately compromising the model's efficacy.

# 5 RELATED WORK

Existing research has investigated the characteristics of NFTs, including attributes extracted from their metadata. These studies have investigated features such as rarity, creator information, and on-chain activities, analyzing key attributes, trends, and challenges associated with successful NFT products [32]. Collectible digital works and creative artworks have been identified as the most attractive NFT categories, with discussions encompassing design features, usability challenges, and security concerns [1, 5]. The unique characteristics of NFT collectibles, including functionality, scarcity, aesthetics, and price value, along with the attributes of the blockchain, such as security and privacy, influence both utilitarian and hedonistic attitudes toward NFTs. These factors collectively shape purchase intentions [9, 24].

Furthermore, additional studies have focused on analyzing NFT marketplaces. NFT exchanges can occur between previously anonymous counterparties since payment and asset transfer happen atomically in a single operation [4]. These investigations have explored various properties of NFT sales, including statistical characteristics, visual features, and predictability, offering insights into the structure and evolution of the NFT market [21].

Recommender systems refer to technologies that utilize various algorithms to provide users with personalized suggestions of potentially relevant information or products, based on analysis of data regarding their historical behaviors, expressed interests, preferences, and more [20]. Since their emergence in the 1990s, recommender systems have become widely studied and deployed across diverse online platforms and services, rapidly advancing in sophistication, diversity, and performance [8].

Extensive research has been dedicated towards Recommender systems across academia and industry, with widespread real-world implementation demonstrating their capabilities in providing value for both users and providers. Successful examples can be observed within numerous domains, including e-commerce, social networking, media streaming, search engines, and more [26]. Major online retailers such as Amazon and Alibaba leverage recommendations to enable personalized discoveries that enhance user experiences and drive sales [18, 29]. Social media platforms including TikTok and Instagram deliver customized content feeds to cater to user interests and further boost engagement [16, 22, 33]. Netflix, YouTube, and other media services optimize suggestions to match individual viewing tastes and increase consumption [7, 10]. Web search engines like Google also incorporate personalization into search rankings and advertising to improve click-through rates [19].

However, recommendations remain relatively unexplored within emerging domains such as NFTs, which have gathered substantial recent interest. Multiple factors may contribute to scarce NFT recommendation research. Firstly, NFTs only gained wider public awareness and adoption in the past couple of years, with market expansion still at its early stages [3]. Secondly, the inherent uniqueness and scarcity of each NFT artwork pose challenges for conventional recommendation approaches centered around commodities and generalized user preferences. More tailored techniques would need to take into account nuanced traits of discrete NFT items. As activity within NFT platforms and metaverses accumulates over time alongside community maturity, dedicated Recommender systems may emerge to match entities to users or scenarios.

# 6 CONCLUSION

Inspired by the efficiency of intent-driven interaction patterns in blockchain markets, we model user purchasing behavior from an intent perspective to address the challenge of high personalization in NFT markets, which traditional recommendation systems struggle to accommodate. In this paper, we propose IHRL (Intent-aware Hypergraph Representation Learning), a novel method for NFT recommendation. We introduce disentanglement techniques to separate and identify user purchasing patterns under different intents, enabling the model to capture diverse buying motivations more precisely. Additionally, we design a hypergraph learning module to explore higher-order correlations among NFTs. Our attention-based convolutional network not only aggregates features of multiple NFTs within a single user purchase but also facilitates effective information transfer across different purchasing behaviors. We conducted extensive evaluations on a large-scale dataset comprising over 2.6 million Ethereum NFT transactions. The results demonstrate that IHRL significantly outperforms existing state-of-the-art baseline methods, confirming the applicability and effectiveness of our approach in the NFT domain.

Future research directions include exploring IHRL's adaptability to other blockchain networks and investigating its potential applications in related fields such as Decentralized Finance (DeFi), Social Finance (SocialFi), and Game Finance (GameFi).

# References


[1] Omar Ali, Mujtaba Momin, Anup Shrestha, Ronnie Das, Fadia Alhajj, and Yogesh K. Dwivedi. 2023. A Review of the Key Challenges of Non-Fungible Tokens. *Technological Forecasting and Social Change* 187 (Feb. 2023), 122248. https://doi.org/10.1016/j.techfore.2022.122248

[2] Giulio Anselmi and Giovanni Petrella. 2023. Non-fungible token artworks: More crypto than art? *Finance research letters* 51 (2023), 103473.

[3] Lennart Ante. 2023. Non-Fungible Token (NFT) Markets on the Ethereum Blockchain: Temporal Development, Cointegration and Interrelations. *Economics of Innovation and New Technology* 32, 8 (Nov. 2023), 1216–1234. https://doi.org/10.1080/10438599.2022.2119564

[4] Sangam Bhujel and Yogachandran Rahulamathavan. 2022. A Survey: Security, Transparency, and Scalability Issues of NFT's and Its Marketplaces. *Sens.* 22, 22 (Nov. 2022), 8833. https://doi.org/10.3390/s22228833

[5] Claudio Boido and Mauro Aliano. 2023. Digital Art and Non-Fungible-Token: Bubble or Revolution? *Finance Research Letters* 52 (March 2023), 103380. https://doi.org/10.1016/j.frl.2022.103380

[6] Anatoli Colicev. 2023. How can non-fungible tokens bring value to brands. *International Journal of Research in Marketing* 40, 1 (2023), 30–37.

[7] Paul Covington, Jay Adams, and Emre Sargin. 2016. Deep Neural Networks for YouTube Recommendations. In *Proceedings of the 10th ACM Conference on*

*Recommender Systems* (Boston, Massachusetts, USA) *(RecSys '16)*. Association for Computing Machinery, New York, NY, USA, 191–198. https://doi.org/10.1145/2959100.2959190

[8] Yashar Deldjoo, Fatemeh Nazary, Arnau Ramisa, Julian McAuley, Giovanni Pellegrini, Alejandro Bellogin, and Tommaso Di Noia. 2023. A Review of Modern Fashion Recommender Systems. *Comput. Surveys* 56, 4 (Oct. 2023), 87:1–87:37. https://doi.org/10.1145/3624733

[9] Marius Arved Fortagne and Bettina Lis. 2024. Determinants of the purchase intention of non-fungible token collectibles. *Journal of Consumer Behaviour* 23, 2 (2024), 1032–1049.

[10] Carlos A. Gomez-Uribe and Neil Hunt. 2016. The Netflix Recommender System: Algorithms, Business Value, and Innovation. *ACM Trans. Manage. Inf. Syst.* 6, 4 (Dec. 2016), 13:1–13:19. https://doi.org/10.1145/2843948

[11] Xiangnan He, Kuan Deng, Xiang Wang, Yan Li, Yongdong Zhang, and Meng Wang. 2020. Lightgcn: Simplifying and powering graph convolution network for recommendation. In *Proceedings of the 43rd International ACM SIGIR conference on research and development in Information Retrieval*. ACM, Association for Computing Machinery, 639–648.

[12] Balázs Hidasi, Alexandros Karatzoglou, Linas Baltrunas, and Domonkos Tikk. 2015. Session-based recommendations with recurrent neural networks. *arXiv e-prints* (2015), arXiv–1511.

[13] Yupeng Hou, Binbin Hu, Zhiqiang Zhang, and Wayne Xin Zhao. 2022. CORE: Simple and Effective Session-based Recommendation within Consistent Representation Space. In *Proceedings of the 45th International ACM SIGIR Conference on Research and Development in Information Retrieval* (<conf-loc>, <city>Madrid</city>, <country>Spain</country>, </conf-loc>) *(SIGIR '22)*. Association for Computing Machinery, New York, NY, USA, 1796–1801. https://doi.org/10.1145/3477495.3531955

[14] Eder John Scheid. 2022. *An intent-based blockchain-agnostic interaction environment.* Ph. D. Dissertation. University of Zurich.

[15] Wang-Cheng Kang and Julian McAuley. 2018. Self-attentive sequential recommendation. In *2018 IEEE international conference on data mining (ICDM)*. IEEE, 197–206.

[16] Hyeyoung Ko, Suyeon Lee, Yoonseo Park, and Anna Choi. 2022. A Survey of Recommendation Systems: Recommendation Models, Techniques, and Application Fields. *Electronics* 11, 1 (2022), 141. https://doi.org/10.3390/electronics11010141

[17] Logan Kugler. 2021. Non-Fungible Tokens and the Future of Art. *Commun. Acm* 64, 9 (Sept. 2021), 19–20. https://doi.org/10.1145/3474355

[18] G. Linden, B. Smith, and J. York. 2003. Amazon.Com Recommendations: Item-to-Item Collaborative Filtering. *IEEE Internet Computing* 7, 1 (Jan. 2003), 76–80. https://doi.org/10.1109/MIC.2003.1167344

[19] Qi Liu, Haiping Ma, Enhong Chen, and Hui Xiong. 2013. A Survey of Context-Aware Mobile Recommendations. *Int. J. Info. Tech. Dec. Mak.* 12, 01 (Jan. 2013), 139–172. https://doi.org/10.1142/S0219622013500077

[20] Linyuan Lü, Matúš Medo, Chi Ho Yeung, Yi-Cheng Zhang, Zi-Ke Zhang, and Tao Zhou. 2012. Recommender Systems. *Physics Reports* 519, 1 (Oct. 2012), 1–49. https://doi.org/10.1016/j.physrep.2012.02.006

[21] Matthieu Nadini, Laura Alessandretti, Flavio Di Giacinto, Mauro Martino, Luca Maria Aiello, and Andrea Baronchelli. 2021. Mapping the NFT Revolution: Market Trends, Trade Networks, and Visual Features. *Sci. Rep.* 11, 1 (Oct. 2021), 20902. https://doi.org/10.1038/s41598-021-00053-8

[22] Changhua Pei, Yi Zhang, Yongfeng Zhang, Fei Sun, Xiao Lin, Hanxiao Sun, Jian Wu, Peng Jiang, Junfeng Ge, Wenwu Ou, and Dan Pei. 2019. Personalized Re-Ranking for Recommendation. In *Proceedings of the 13th ACM Conference on Recommender Systems (RecSys '19)*. Association for Computing Machinery, New York, NY, USA, 3–11. https://doi.org/10.1145/3298689.3347000

[23] Dinuka Piyadigama and Guhanathan Poravi. 2022. An Analysis of the Features Considerable for NFT Recommendations. In *2022 15th International Conference on Human System Interaction (HSI)*. 1–7. https://doi.org/10.1109/HSI55341.2022.9869497

[24] Dhanya Pramod, Vijayakumar Bharathi S, and Kanchan Pranay Patil. 2024. Tokenizing Tangible Intentions: Unraveling the Motives to Try NFTs. *Journal of Computer Information Systems* (2024), 1–14.

[25] A. Rabaai, S. Maati, N. Muhammad, and E. Eljamal. 2024. Barriers to Invest in NFTs: An Innovation Resistance Theory Perspective. *Uncertain Supply Chain Management* 12, 1 (2024), 610–614.

[26] Brent Smith and Greg Linden. 2017. Two Decades of Recommender Systems at Amazon. com. *IEEE Internet Computing* 21, 03 (2017), 12–18.

[27] Qiaoyu Tan, Jianwei Zhang, Jiangchao Yao, Ninghao Liu, Jingren Zhou, Hongxia Yang, and Xia Hu. 2021. Sparse-interest network for sequential recommendation. In *Proceedings of the 14th ACM international conference on web search and data mining*. 598–606.

[28] Ashish Vaswani, Noam Shazeer, Niki Parmar, Jakob Uszkoreit, Llion Jones, Aidan N. Gomez, Lukasz Kaiser, and Illia Polosukhin. 2017. Attention Is All You Need. In *Proceedings of the 31st International Conference on Neural Information Processing Systems (NIPS'17)*. Curran Associates Inc., 6000–6010. https://doi.org/10.5555/3295222.3295349

[29] Jizhe Wang, Pipei Huang, Huan Zhao, Zhibo Zhang, Binqiang Zhao, and Dik Lun Lee. 2018. Billion-Scale Commodity Embedding for E-Commerce Recommendation in Alibaba. In *Proceedings of the 24th ACM SIGKDD International Conference on Knowledge Discovery & Data Mining* (London, United Kingdom) *(KDD '18)*. Association for Computing Machinery, New York, NY, USA, 839–848. https://doi.org/10.1145/3219819.3219869

[30] Qin Wang, Rujia Li, Qi Wang, and Shiping Chen. 2021. Non-Fungible Token (NFT): Overview, Evaluation, Opportunities and Challenges. arXiv:2105.07447 [cs]

[31] Qin Wang, Rujia Li, Qi Wang, and Shiping Chen. 2021. Non-fungible token (NFT): Overview, evaluation, opportunities and challenges. *arXiv preprint arXiv:2105.07447* (2021).

[32] Chih-Hung Wu, Chien-Yu Liu, and Ting-Sheng Weng. 2023. Critical factors and trends in NFT technology innovations. *Sustainability* 15, 9 (2023), 7573.

[33] Min Zhang and Yiqun Liu. 2021. A Commentary of TikTok Recommendation Algorithms in MIT Technology Review 2021. *Fundamental Research* 1, 6 (2021), 846–847. https://doi.org/10.1016/j.fmre.2021.11.015

# A Data Extraction

The Seaport protocol's extensible design allows for multiple items in both the buyer's bid (referred to as "consideration" in Seaport) and the seller's offer. To facilitate subsequent machine learning analysis, we standardized the charge unit for each item. Reflecting the cryptocurrency-centric perspective prevalent among crypto investors, we denominated all prices in ETH (Ethereum's native token). ETH was chosen due to its status as the second-largest cryptocurrency by market capitalization and its widespread use in the Web3 industry. For transactions involving other fungible tokens, we converted their values to ETH equivalents based on the exchange rates on the day of each transaction. To determine the ETH amount of each bid, we parsed the token information (both ETH and ERC20) from the buyer's bid content and combined this with relevant exchange rate data. This approach allowed us to flatten the complex, multi-item transaction data into a unified format, using ETH as the common denominator. This standardization not only simplifies our data structure but also aligns with the predominant value perspective in the crypto ecosystem. Table 4 shows transaction features considered in this study. And we conducted features for each NFT item, as shown in Table 5.

Due to the failure of many NFT off-chain data parsing processes caused by external factors such as expired URLs, we consulted NFT industry experts and conducted actual market research, which led us to believe that most of these NFTs are fraudulent and scam-related. Therefore, we consider this portion of data as anomalous and should be removed.

**Table 2: Impact of the Different Number of Intents.**

| Number of Intents | Recall (%) | | | | MRR (%) | | | | IC (%) | | | |
|---|---|---|---|---|---|---|---|---|---|---|---|---|
| K | 5 | 10 | 15 | 20 | 5 | 10 | 15 | 20 | 5 | 10 | 15 | 20 |
| 1 | 55.49 | 64.84 | 68.52 | 71.63 | 44.38 | 45.67 | 45.96 | 46.14 | 14.62 | 21.41 | 26.43 | 30.95 |
| 2 | 56.97 | 65.98 | 69.38 | 72.60 | 46.32 | 47.60 | 47.87 | 48.05 | 15.00 | 22.10 | 27.77 | 32.49 |
| 4 | 60.86 | 68.17 | 72.54 | 74.65 | 51.82 | 52.80 | 53.15 | 53.27 | 15.00 | 23.37 | 29.88 | 35.40 |
| 5 | 74.04 | 79.42 | 81.48 | 82.78 | 63.91 | 64.63 | 64.80 | 64.86 | 30.78 | 47.26 | 58.18 | 65.67 |
| 8 | 60.26 | 66.25 | 70.33 | 72.82 | 50.43 | 51.23 | 51.55 | 51.69 | 14.12 | 22.39 | 28.84 | 34.58 |

**Table 3: Impact of Embedding Dimension Size.**

| Dimension Size | Recall (%) | | | | MRR (%) | | | | IC (%) | | | |
|---|---|---|---|---|---|---|---|---|---|---|---|---|
| d | 5 | 10 | 15 | 20 | 5 | 10 | 15 | 20 | 5 | 10 | 15 | 20 |
| 80 | 52.41 | 61.52 | 66.19 | 69.38 | 43.14 | 44.38 | 44.75 | 44.93 | 13.03 | 20.49 | 26.52 | 31.72 |
| 160 | 56.94 | 64.18 | 68.94 | 71.66 | 45.58 | 46.55 | 46.92 | 47.08 | 14.20 | 22.15 | 28.39 | 33.93 |
| 320 | 74.04 | 79.42 | 81.48 | 82.78 | 63.91 | 64.63 | 64.80 | 64.86 | 30.78 | 47.26 | 58.18 | 65.67 |
| 640 | 58.82 | 65.63 | 69.28 | 72.38 | 49.64 | 50.56 | 50.85 | 51.02 | 14.50 | 22.81 | 29.38 | 34.96 |

**Table 4: Collected NFT Transactions (2,613,617 NFT trading orders in total)**

| Columns | Descriptions |
|---|---|
| user_id | The NFT buyer's address on the blockchain |
| item_id | The unique id of NFT, represented by combining the collection address and NFT ID |
| timestamp | The block number of the transaction occurrence |
| timestamp | The timestamp of the block number when the transaction occurrence |
| total_value | The total value of ETH in the (raw) bundled transaction. |

**Table 5: Collected NFT Item Data (2,130,719 NFT Item in total)**

| Column | Descriptions |
|---|---|
| item_id | The unique ID of NFT, represented by combining the collection address and NFT ID (usually a unit256) |
| collection_id | The unique ID of NFT collection, represented by the collection address |
| collection_name | The name of the collection to which the NFT belongs |
| collection_symbol | The symbol of the collection to which the NFT belongs |
| historical_count | The total number of purchases for the NFT item across all its orders |
| historical_prices | A sequence of the NFT item's historical purchase prices from its orders denominated in ETH |